Chemical Physics Letters 474 (2009) 185–189

Contents lists available at ScienceDirect

Chemical Physics Letters

journal homepage: www.elsevier.com/locate/cplett

An experimental and theoretical description of the $(NH_3)_{n-1}\{NH_3–H–H_2O\}^+$ cluster ions produced by fast ion bombardment

Francisco Alberto Fernandez-Lima [a], Thiago Messias Cardozo [b], Enio Frota da Silveira [c], Marco Antonio Chaer Nascimento [b,*]

[a] Department of Chemistry, Texas A&M University, College Station, TX, USA
[b] Instituto de Química, Universidade Federal do Rio de Janeiro, Cidade Universitária, CT Bloco A sala 412, Rio de Janeiro 21949-900, RJ, Brazil
[c] Departamento de Física, Pontifícia Universidade Católica, Rio de Janeiro, Brazil

ARTICLE INFO

Article history:
Received 19 March 2009
In final form 19 April 2009
Available online 22 April 2009

ABSTRACT

The $(NH_3)_{n-1}\{NH_3–H–H_2O\}^+$ cluster series produced by ^{252}Cf fission fragments (FF) impact onto a $NH_3–H_2O$ ice target have been analyzed theoretically and experimentally. The ion desorption yields show a smooth dependence of the cluster population on its mass, with a relative higher abundance for $n = 3$. Results of DFT calculations show that two main series of cluster ions may be formed corresponding to the $\{H_3O\}^+$ and $\{NH_4H_2O\}^+$ cores. The theoretical analysis shows that the members of the $(NH_3)_{n-1}\{NH_4–H_2O\}^+$ series are more stable than those of the $(NH_3)_n\{H_3O\}^+$ series, the $(NH_3)_2\{NH_3–H–H_2O\}^+$ structure being the most stable one, in agreement with the experiments.

1. Introduction

The study of molecular clusters in the gas phase and solid state has been the focus of large number of investigations over the last decades, specially motivated by the differences in the chemical and physical properties as the cluster decreases in size and start to behave less like the bulk material. Investigation on the formation of ammonia or water clusters are of particular interest since they provide insight into the nature of hydrogen bonded systems not only in the gaseous state but also in the liquid and solid phases. Recently, several theoretical and experimental investigations on hydrogen-bonded molecular clusters of polar molecules, especially water and ammonia containing clusters, have been reported [1–11].

Clustering processes involving ammonium and hydronium ions are relevant not only from the physical–chemical fundamental aspects but also because they are supposed to occur in ionized planetary atmospheres, interstellar clouds and cosmic icy surfaces [12,13]. Ammonium and hydronium ions as well as ammonia and water have relatively simple molecular structures, well established chemical behavior, constituting therefore appropriate prototypical systems for studying the proton transfer phenomenon [14–22]. However, the available experimental data on mixed series is scarce mainly because of the predominant strongly bonded nature of the pure ammonia and water cluster series [23–27].

Mass spectrometry studies are necessary in order to investigate the dependence of the cluster abundance on their masses. To this purpose, ionized cluster species must be produced from their neutral gas or solid phases. For example, the generation of positively charged ammonia clusters has been performed using several ionization techniques, such as multiphoton ionization, single photon ionization, electron impact ionization and ultrafast pump-probe techniques. In a previous Letter, where positive and negatively charged water $[(H_2O)_nH_3O^+, (H_2O)_nOH^-]$ and ammonia $[(NH_3)_n-NH_4^+(NH_3)_nNH_2^-]$ cluster series were examined, we described the advantages of using fast ion bombardment of ice surfaces to generate charged cluster ion distributions [23,24,28]. We have also showed [23,24,28] that the relative abundances observed in the mass spectra can be related to the cluster stabilities, and that ab initio calculations including electron correlation effects can provide an accurate description of the most stable candidate structures [29–33].

Although studies on positively and negatively charged ammonia and water clusters have been reported, to our knowledge a comprehensive and detailed characterization of the $(NH_3)_{n-1}\{NH_3–H–H_2O\}^+$ series has not yet been performed. This Letter reports the characterization of the $(NH_3)_{n-1}\{NH_3–H–H_2O\}^+$ cluster series produced by a ^{252}Cf fission fragment (FF) impact onto a $NH_3–H_2O$ ice target. The $(NH_3)_{0-5}[NH_3–H–H_2O]^+$ members have been theoretically and experimentally analyzed. In particular, we are interested in describing the correlation between the cluster stability and the relative cluster populations in the mass spectra. The observed results are discussed and an attempt at interpreting the spectra is made based on a search for the more stable conformers using Density Functional Theory at the B3LYP and X3LYP levels of calculation with an extended basis set.

* Corresponding author. Fax: +55 21 2562 7265.
E-mail address: chaer@iq.ufrj.br (M.A.C. Nascimento).

0009-2614/$ - see front matter © 2009 Elsevier B.V. All rights reserved.
doi:10.1016/j.cplett.2009.04.054

2. Experimental

The experimental features of ^{252}Cf-PDMS analysis on condensed gases can be found elsewhere [23,24,28]. Briefly, an NH_3–H_2O ice target was grown by condensation of a NH_3–H_2O gas mixture over an Au substrate at controlled low temperature (in the 30–40 K range). A fission fragment (FF) produced by a ^{252}Cf source eventually collides with the NH_3–H_2O ice target inducing ion desorption in high vacuum conditions (in the low 10^{-8} mbar). The desorbed ions are accelerated by an extraction field into a field-free region and are detected by a micro channel plate detector. The mass analysis is performed by the time-of-flight technique (TOF) [34]. The typical mass-resolving power in the current spectra is about $m/\Delta m \sim 200$ for the worst case and the m/z of interest are completely resolved.

The ^{252}Cf FF impact induces desorption of positive and negative ions, as well of neutral particles. A typical TOF mass spectrum of positively charged species produced when the NH_3–H_2O ice target, with a low concentration of H_2O, is bombarded by ^{252}Cf FF is presented in Fig. 1 (top). The secondary ion emission consists of three main series: $(NH_3)_{n-1}\{NH_3\text{–}H\text{–}H_2O\}^+$, $(H_2O)_nH_3O^+$ and $(NH_3)_nNH_m^+$. The desorption yields $Y(n)$ of the members of the $(NH_3)_{n-1}\{NH_3\text{–}H\text{–}H_2O\}^+$ series varies smoothly with the cluster size, n, and a relative higher abundance is observed for the $(NH_3)_2\{NH_3\text{–}H\text{–}H_2O\}^+$ cluster ion compared to the other members of the series (Fig. 1 bottom). The relative higher abundance of the $(NH_3)_4NH_4^+$ member of the $(NH_3)_nNH_4^+$ series is also noticeable. The predominant, strongly bonded $(NH_3)_nNH_m^+$ and $(H_2O)_nH_3O^+$ series have been described in previous reports [23,24] and will not be discussed here.

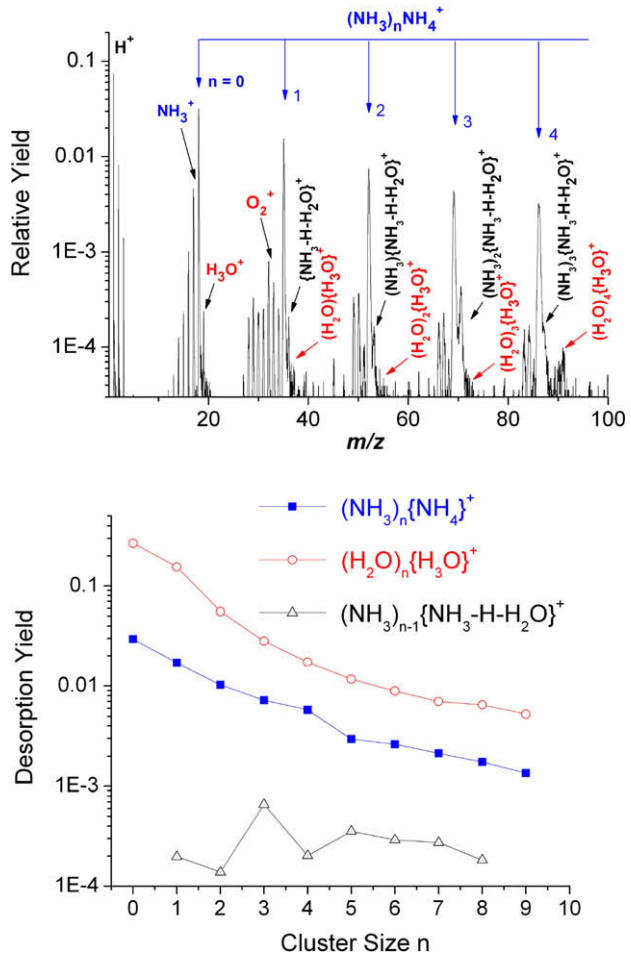

Fig. 1. (Top) Positive time-of-flight mass spectrum of the H_2O–NH_3 ice target, with low concentration of H_2O, bombarded by ^{252}Cf fission fragments. (Bottom) Relative secondary ion yields of $(NH_3)_{n-1}\{NH_3\text{–}H\text{–}H_2O\}^+$ series out of a H_2O–NH_3 mixture ice target with low concentration of H_2O, and $(H_2O)_nH_3O^+$ and $(NH_3)_nNH_4^+$ series out of pure H_2O and NH_3 ice targets, respectively. Notice the relative higher abundance of the $(NH_3)_2\{NH_3\text{–}H\text{–}H_2O\}^+$ cluster ion with respect to the other members of the series.

3. Computational details

Theoretical calculations have been performed with the purpose of determining the most stable structures of the $(NH_3)_{n-1}\{NH_3\text{–}H\text{–}H_2O\}^+$ cluster ions and of investigating if the cluster properties (e.g., stability, charge distribution and binding energy) could be directly related to the relative abundances observed in the mass spectra. To obtain a description of the NH_3 units attached to the hydronium or ammonium ions, Density Functional Theory (DFT) calculations were performed using the B3LYP and X3LYP functionals with the 6-311G**++ and cc-PVTZ(-f)++basis sets. A vibration analysis was performed for all the obtained structures at the level of calculation employed. No symmetry restrictions or any other kind of constraints have been imposed during the process of geometry optimization. B3LYP and other functionals do not give an accurate description of neutral systems interacting through hydrogen-bond or dispersion-type forces, although with the advent of the X3LYP functional the description of such systems has been considerably improved. However, in the case of charged species, the interaction is dominated by electrostatic forces which are much better described at the DFT level. The vibrational analysis of the optimized structures showed that the DFT/X3LYP functional gives a better representation of the $(NH_3)_{n-1}\{NH_3\text{–}H\text{–}H_2O\}^+$ system compare to the DFT/B3LYP functional and, therefore, the X3LYP results were used for further analysis.

It is also well-known that DFT calculations may be in error due to the fact that, for the present available functionals, the exchange energy does not exactly cancel the Coulombic self-interaction and that this effect is more pronounced for charged species [35]. On the other hand, this effect becomes less important as the size of the ions increase. To check for possible inconsistencies, the smaller structures were also optimized using the Möller–Plesset (MP) perturbation theory, at the MP2/6-311G**++level of calculation. No substantial changes were observed either in the geometrical parameters or in the relative stability of the clusters.

All calculations were carried out using the Jaguar 6.0 software (Schrödinger Inc., Portland, OR) [36]. Charge analysis was performed on the optimized structures using the CHelpG algorithm [37].

4. Results and discussion

The search for the most stable structures reveals that two main series of water–ammonium cluster ions can be produced (Fig. 2), corresponding to two distinct $\{NH_3\text{–}H\text{–}H_2O\}^+$ cores, $\{NH_4\text{–}H_2O\}^+$ and $\{NH_3\text{–}H_3O\}^+$, to which the NH_3 units are attached. The similarity of the obtained structures suggests that the mechanism of the cluster formation is strongly related to the formation of the ion cores and the successive attachments of NH_3 neutral units. The charge distribution of the $\{NH_3\text{–}H\text{–}H_2O\}^+$ free cores were found to be $NH_4^{+1.03}$—$H_2O^{-0.03}$ and $NH_3^{+0.17}$—$H_3O^{+0.83}$.

The energies of the stable structures are shown in Table 1 together with other properties that will be further discussed at the end of this section.

The relative abundances of the $\{NH_4\text{–}H_2O\}^+$ and $NH_3\{H_3O\}^+$ species depend upon the relative abundances of the NH_4^+ and H_3O^+ cores during the ion desorption process. If NH_3 and H_2O molecules are desorbed with equal probabilities by the ^{252}Cf fission fragment,

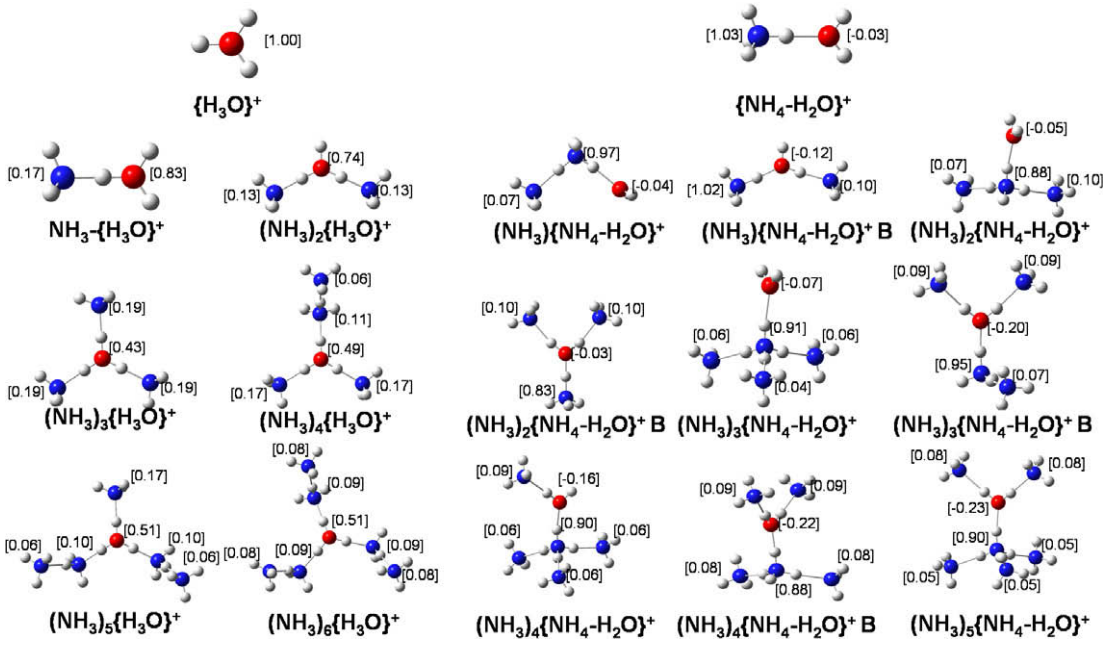

Fig. 2. Optimized geometries of the $(NH_3)_{n-1}\{NH_4–H_2O\}^+$ and $(NH_3)_n\{H_3O\}^+$ series at the DFT/X3LYP/6-311G**++level of calculation. Higher energy isomers observed for the $(NH_3)_{n-1}\{NH_4–H_2O\}^+$ series are labeled B. Partial charges of the NH_3, H_2O, NH_4 and H_3O units are shown in brackets.

which is a reasonable assumption considering the small m/z difference (1 u), then the lower proton affinity of the H_2O molecule (7.16 eV) compared to that of the NH_3 molecule (8.85 eV) makes the formation of H_3O^+ ions less probable. However, if the experimental conditions are such that the abundance of NH_4^+ is much smaller than that of the H_3O^+ ions, then the $(NH_3)_n\{H_3O\}^+$ series may be primarily formed. Nevertheless, the energy barrier for the H_3O^+ to NH_3 proton transfer reaction is relatively small [38]. For distances between the acceptor and donor centers of the order of magnitude observed in the $(NH_3)_n\{H_3O\}^+$ clusters (2.9 Å) the energy barrier is equal to 3.6 kJ mol^{-1} at the MP2/6-31G(d,p) level of calculation [38]. Therefore, the members of that series can be readily converted to the corresponding ones of the more stable $(NH_3)_{n-1}\{NH_4–H_2O\}^+$ series. Previous reports also suggested that the lifetime of the intermediate ion–molecule complex formed upon encountering reactants depends strongly on their initial relative orientation [38,39], i.e., when the proton to be transferred is properly lined-up between oxygen and nitrogen, rapid transfer occurs. In the case of the ^{252}Cf bombardment experiments, this eventual transition can occur just in the first moments of the desorption process because of the rapid decreased in density of the desorbed molecules as the expansion process develops. On the other hand, the relative abundances of each series may also depend on the H_2O:NH_3 mixture ratio in the ice target and this will be discussed in a future Letter.

Table 1
Energy (E), deviation energy (D_n, see text) and binding energy (BE) of the stable clusters at the DFT/X3LYP/6-311G**++level of calculation.

DFT/X3LYP/6-311G**++				
n	E (eV)	E + ZPE (eV)	D_n (eV)	BE (eV)
$(NH_3)_n\{H_3O\}^+$				
1	−3627.84	−3625.90	0.97	1.69
2	−5168.26	−5165.60	−0.13	1.71
3	−6708.29	−6704.32	−0.25	0.74
4	−8247.70	−8242.69	−0.01	0.38
5	−9787.07	−9781.05	0.23	0.37
6	−11326.42	−11319.38	0.51	0.34
$(NH_3)_{n-1}\{NH_4–H_2O\}^+$				
1	−3628.82	−3626.81	−0.06	0.89
2	−5168.73	−5165.71	−0.24	0.91
3	−6708.42	−6704.38	−0.31	0.68
4	−8247.97	−8242.92	−0.24	0.55
5	−9787.50	−9781.41	−0.12	0.51
6	−11326.87	−11319.77	0.11	0.44
$(NH_3)_{n-1}\{NH_4–H_2O\}^+B$				
2	−5168.61	−5165.60	−0.13	0.8
3	−6708.29	−6704.31	−0.24	0.73
4	−8247.89	−8242.82	−0.14	0.52
5	−9787.44	−9781.34	−0.06	0.54
Others				
NH_4^+	−1548.09	−1546.75		
NH_3	−1538.92	−1537.99		
H_3O^+	−2087.11	−2086.22		
H_2O	−2079.75	−2079.17		

The observation of either series depends on the dynamics of the interconversion and of the ion relaxation process. Considering that the time scale of the TOF experiment ($\sim 10^{-6}$ s) is much larger than the time scale for the ionic clusters formation and its reorganization and fragmentation ($\sim 10^{-14}$–10^{-13} s), it is quite reasonable to assume that the ions being detected (the ones formed during time interval of $\sim 10^{-8}$–10^{-7} s) correspond to the thermodynamically more stable species.

The obtained structures can be classified by their conformational similarities or, as previously proposed, by means of an energy criterion relating the total DFT energy of a particular structure to the average DFT energy across all the structures [29–33]. This taxonomic exercise consists of logically conciliating these different types of sorting. Let $E_n(i)$ be the total DFT energy (including the zero-point energy correction at the DFT/X3LYP/6-311G**++level) of the ith isomer of the $(NH_3)_{n-1}\{NH_3–H–H_2O\}^+$ cluster ion with size n, and $\overline{E}\,(n)$ the average DFT energy of all n-isomers as a function of the cluster size n. The $\overline{E}\,(n)$ function shows a linear dependence on n, as depicted in the inset of Fig. 3: $\overline{E}\,(n) = 2088.26 - 1538.60\ n$. For each isomer, the deviation energy D is defined as $D_n(i) = E_n(i) - \overline{E}(n)$ (Table 1). Lower $D_n(i)$ values are associated with lower energy isomers and thus more stable

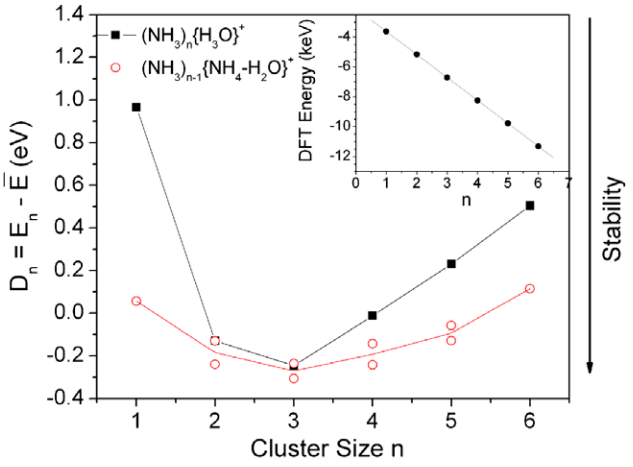

Fig. 3. Deviation plot of the total energy of the clusters as a function of the cluster size (n) at the DFT/X3LYP/6-311G**++level. In the inset, the total DFT energy E_n as a function of the cluster size. Data is given in Table 1.

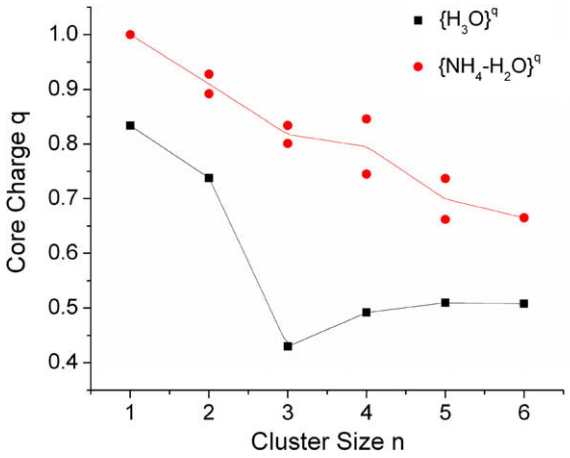

Fig. 5. Core charge q (in e units) as a function of the cluster size (n). For $\{NH_4–H_2O\}^q$, $\{NH_4\}^q$ and $\{H_2O\}^q$ the members are denoted according to the $(NH_3)_{n-1}\{NH_4–H_2O\}^+$ notation.

structures [29–33]. The most relevant aspect of the deviation energy plot (D-plot) is that the more stable isomers can be easily identified to facilitate the analysis of the relative stability.

Fig. 3 shows the $D_n(i)$ values of the obtained structures at the DFT/X3LYP/6-311G**++level of calculation. The structures can be classified into two main series: (i) structures with the ammonium core $(NH_3)_{n-1}\{NH_4–H_2O\}^+$, and (ii) structures with the hydronium core $(NH_3)_n\{H_3O\}^+$. The energy values and the D-plot analysis show that the members of the $(NH_3)_{n-1}\{NH_4–H_2O\}^+$ series are more stable than the corresponding ones of the $(NH_3)_n\{H_3O\}^+$ series. Moreover, for both series the cluster ion with $n = 3$ presents the highest stability, in perfect agreement with the highest abundance observed in the TOF spectra (Fig. 1). The higher energy isomers of the $(NH_3)_{n-1}\{NH_4–H_2O\}^+$ series (label B in Fig. 2) are also more stable than the corresponding members of the $(NH_3)_n\{H_3O\}^+$ series.

The highest stability of the $n = 3$ clusters can be related to their shell structure. From Fig. 2 it is clear that for $n = 3$ the clusters exhibit a closed shell structure characterized by a maximum number of ligands at a minimum distance from the core and disposed spatially as to exhibit a minimum steric repulsion among them. This sort of structure provides maximum stabilization of the core charge with a minimum of steric repulsion. This shell effect has been previously observed in other kinds of clusters [40].

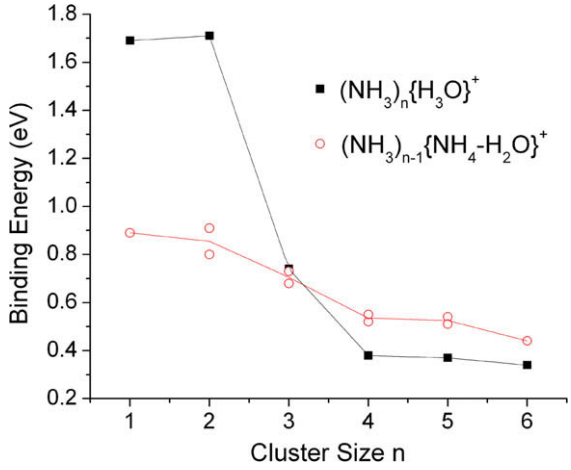

Fig. 4. Binding energy (BE) dependence of the cluster size n at the DFT/X3LYP/6-311G**++level. Data is given in Table 1.

The cluster ion stability can also be related to two quantities: the binding energy (BE, as defined below), and the cluster geometry which are, of course, closely related. The binding energies (BE) were calculated considering the reactions:

$$(NH_3)_{n-1}(H_2O)\{NH_4\}^+ \rightarrow (NH_3)_{n-2}\{NH_4 - H_2O\}^+ + NH_3 \quad (1)$$

$$(NH_3)_n\{H_3O\}^+ \rightarrow (NH_3)_{n-1}\{H_3O\}^+ + NH_3 \quad (2)$$

Fig. 4 shows the BE dependence on the cluster size for the obtained structures. The binding in both series is essentially due to electrostatic forces. The $\{NH_4–H_2O\}^+$ and $\{H_3O\}^+$ cores polarize the NH_3 neutral units, resulting in a net attractive force that binds these units to the central core. The closer the NH_3 unit is to core, the stronger the attractive force should be. However, as the number of NH_3 units increases, steric effects start to play a role in determining how close from the central core each subsequent unit can be placed. The contribution of steric effects can be inferred from the decreasing trend in the BE values as the cluster size increases (Fig. 4). Moreover, for n larger than 2, a sharp decrease on the BE values of the $(NH_3)_n\{H_3O\}^+$ series is observed.

Fig. 5 shows the core charge for the $(NH_3)_{n-1}\{NH_4–H_2O\}^+$ and $(NH_3)_n\{H_3O\}^+$ series as a function of the cluster size. For both series, the core charge decreases as the cluster size increases. The fact that the charge of the $\{NH_4–H_2O\}^+$ core is always higher than that of the $\{H_3O\}^+$ core certainly contributes to the higher stability of the $(NH_3)_{n-1}\{NH_4–H_2O\}^+$ series. For the case of the $(NH_3)_n\{H_3O\}^+$ series, a sharp decrease is observed in the $\{H_3O\}^+$ core charge at $n = 3$ implying that further NH_3 units would be less attached to the core, in good agreement with the sharp decrease observed in the BE values in Fig. 4.

5. Conclusions

The $(NH_3)_{n-1}\{NH_3–H–H_2O\}^+$ cluster ions produced by ^{252}CF impact onto a $NH_3–H_2O$ ice target have been analyzed theoretically and experimentally. The desorption yields show a smooth dependence of the cluster population on its mass, revealing a relative higher abundance at $n = 3$. The DFT/B3LYP and DFT/X3LYP calculations show that two main series of ammonium clusters can be produced. Similar results are obtained at the MP2 level of calculation for the smaller structures. Both series follow a clear pattern: each additional NH_3 group makes a new hydrogen bond with one of the hydrogen atoms of the respective $\{H_3O\}^+$ and $\{NH_4H_2O\}^+$ cores. The D-plot analysis shows that the obtained structures can be classified by their conformational similarities or, within a better

taxonomical description, by their total internal energy. The energy analysis indicates that the members of the $(NH_3)_{n-1}\{NH_4H_2O\}^+$ series are more stable than those of the $(NH_3)_n\{H_3O\}^+$ series. The trend on the relative stability of the $(NH_3)_{n-1}\{NH_4H_2O\}^+$, presents excellent agreement with the experimental distribution of cluster abundances, with the $(NH_3)_2\{NH_4H_2O\}^+$ structure being the most stable. The core charges and the shell analyses are also consistent with the energy analysis.

Acknowledgments

The authors would like to acknowledge the Brazilian Agencies CNPq and Faperj, for their partial support.

References

[1] E.S. Kryachko, Chem. Phys. Lett. 272 (1997) 132.
[2] K. Jongseob, D. Majumdar, L.H. Myoung, S.K. Kwang, J. Chem. Phys. 110 (1999) 9128.
[3] M. Antolovich, L.F. Lindoy, J.R. Reimers, J. Phys. Chem. A 108 (2004) 8434.
[4] M.A.S. Dayle, S. Johan, E. Yasser, A. Ludwik, J. Chem. Phys. 109 (1998) 1238.
[5] A. Lenz, L. Ojamae, Phys. Chem. Chem. Phys. 7 (2005) 1905.
[6] J.A. Odutola, T.R. Dyke, B.J. Howard, J.S. Muenter, J. Chem. Phys. 70 (1979) 4884.
[7] P.M. Pawlowski, S.R. Okimoto, F.M. Tao, J. Phys. Chem. A 107 (2003) 5327.
[8] F. Schulz, B. Hartke, Phys. Chem. Chem. Phys. 5 (2003) 5021.
[9] S. Sefik, A. Lester, J. Chem. Phys. 87 (1987) 5131.
[10] A.L. Sobolewski, W. Domcke, Phys. Chem. Chem. Phys. 7 (2005) 970.
[11] A.K. Sudhir, J.B. Libero, K.P. Rajeev, J. Chem. Phys. 113 (2000) 2697.
[12] L.S. Farenzena et al., Earth Moon Planets 97 (2005) 311.
[13] E. Herbst, Ann. Rev. Phys. Chem. 46 (1995) 27.
[14] R. Mabourki, Y. Ibrahim, E. Xie, M. Meot-Ner, M.S. El-Shall, Chem. Phys. Lett. 424 (2006) 257.
[15] L. Yue, M.F. James, J. Chem. Phys. 120 (2004) 199.
[16] M. Biczysko, Z. Latajka, Chem. Phys. Lett. 313 (1999) 366.
[17] Y. Li, X. Liu, X. Wang, N. Lou, Chem. Phys. Lett. 276 (1997) 339.
[18] A.A. Viggiano, F. Dale, J.F. Paulson, J. Chem. Phys. 88 (1988) 2469.
[19] A.T. Pudzianowski, J. Chem. Phys. 102 (1995) 8029.
[20] T. Rajamaki, A. Miani, L. Halonen, J. Chem. Phys. 118 (2003) 10929.
[21] H. Shinohara, U. Nagashima, H. Tanaka, N. Nishi, J. Chem. Phys. 83 (1985) 4183.
[22] S.C. Park, K.W. Maeng, T. Pradeep, H. Kang, Angew. Chem. Int. Ed. 40 (2001) 1497.
[23] R. Martinez et al., Int. J. Mass Spectrom. 253 (2006) 112.
[24] V.M. Collado, L.S. Farenzena, C.R. Ponciano, E.F. da Silveira, K. Wien, Surf. Sci. 569 (2004) 149.
[25] G. Hulthe, G. Stenhagen, O. Wennerstroem, C.H. Ottosson, J. Chrom. A 777 (1997) 155.
[26] G.M. Lancaster, F. Honda, Y. Fukuda, J.W. Rabalais, J. Am. Chem. Soc. 101 (1979) 1951.
[27] R. Souda, Nucl. Instrum. Meth. Phys. Res. B 232 (2005) 125.
[28] L.S. Farenzena, V.M. Collado, C.R. Ponciano, E.F. da Silveira, K. Wien, Int. J. Mass Spectrom. 243 (2005) 85.
[29] F.A. Fernández-Lima, C.R. Ponciano, E.F. da Silveira, M.A.C. Nascimento, Chem. Phys. Lett. 445 (2007) 147.
[30] F.A. Fernandez-Lima, C.R. Ponciano, G.S. Faraudo, M. Grivet, E.F. da Silveira, M.A.C. Nascimento, Chem. Phys. 340 (2007) 127.
[31] F.A. Fernández-Lima, T.M. Cardozo, R.M. Rodriguez, C.R. Ponciano, E.F. da Silveira, M.A.C. Nascimento, J. Phys. Chem. A 111 (2007) 8302.
[32] F.A. Fernández-Lima, C.R. Ponciano, E.F. da Silveira, M.A.C. Nascimento, Chem. Phys. Lett. 426 (2006) 351.
[33] F.A. Fernández-Lima, C.R. Ponciano, M.A.C. Nascimento, E.F. da Silveira, J. Phys. Chem. A 110 (2006) 10018.
[34] R.J. Cotter, Time-of-Flight Mass Spectrometry: Instrumentation and Applications in Biological Research, American Chemical Society, Washington, DC, 1997.
[35] R. Notker, S.B. Trickey, J. Chem. Phys. 106 (1997) 8940.
[36] Jaguar 6.0. Schroedinger Inc., Portland, OR, 2004.
[37] C.M. Breneman, K.W. Wiberg, J. Comput. Chem. 11 (1990) 36.
[38] H.H. Bueker, E. Uggerud, J. Phys. Chem. 99 (1995) 5945.
[39] H.H. Bueker, T. Helgaker, K. Ruud, E. Uggerud, J. Phys. Chem. 100 (1996) 15388.
[40] M. Barbatti, G. Jalbert, M.A.C. Nasciemento, J. Chem. Phys. 113 (2000) 4230.